

# One-dimensional Bose gas dynamics: breather relaxation

Bogdan Opanchuk and Peter D. Drummond

*Centre for Quantum and Optical Science, Swinburne University of Technology, Melbourne 3122, Australia*

One-dimensional Bose gases are a useful testing-ground for quantum dynamics in many-body theory. They allow experimental tests of many-body theory predictions in an exponentially complex quantum system. Here we calculate the dynamics of a higher-order soliton in the mesoscopic case of  $N = 10^3 - 10^4$  particles, giving predictions for quantum soliton breather relaxation. These quantum predictions use a truncated Wigner approximation, which is a  $1/N$  expansion, in a regime where other exactly known predictions are recovered to high accuracy. Such dynamical calculations are testable in forthcoming BEC experiments.

Techniques for observing near lossless quantum dynamics have led to quantitative tests of quantum field dynamics in photonic systems [1–4]. Improvements in ultra-cold quantum gas experiments mean that these experiments can now also compare first principles calculations of many-body quantum dynamics with observations [5]. The 1D Bose gas, with its well-understood conservation laws [6] and exact solutions [7, 8] is an excellent testing ground for these ideas. Second-order correlations in thermal equilibrium with repulsive interactions have been predicted [9–11] and verified experimentally [12, 13]. In these systems, there is evidence of steady-states that do not have a Gibbs structure [14, 15]. Attractive matter-wave solitons have also been experimentally observed [16–21].

Here we show that the dynamical stability of higher-order matter-wave solitons prepared by quenching is experimentally testable. Fragmentation and damping of breathing oscillations [22, 23] are predicted to persist even up to a mean particle number of  $N = 1000$ . These calculations use the truncated Wigner approximation, which is a  $1/N$  expansion [24–26]. Known conserved quantities are replicated with high accuracy. This is a regime accessible to current BEC experiments [21, 23, 27]. We show that direct experimental tests of predictions for soliton fragmentation and center-of-mass dynamics are possible in an exponentially complex regime where exact calculation is extremely difficult.

Fragmentation causes a decay in oscillation that is predicted to happen gradually, without the abrupt changes after a short evolution time found by variational methods [28]. Such methods are known to disagree with exact COM spreading results [29], which means that they violate Galilean invariance [30]. This is presumably because the number of dissociation channels is much larger than the number of variational modes used in such calculations. The oscillation decay found here is slower than predicted at very small particle number [22], and also less pronounced than the predicted fragmentation at small  $N$  obtained from exact analysis [23]. However, this general difference is consistent with the scaling we find with  $N$ : where fragmentation and breather relaxation are reduced as  $N$  increases to give mean field behavior at large  $N$ .

The quantum nonlinear Schroedinger equation and its dissipative extensions has been widely used to calculate quantum dynamical properties of Bose gases [31, 32]. This earlier work used phase-space techniques that originate in the work of Wigner [33] and Glauber [34]. Such predictions have been experimentally verified [1, 35, 36]. Here we investigate the dynamics of a higher-order soliton or breather. In this case, even more dramatic effects can occur due to quantum fragmentation. Due to the enormous state-space, direct calculation with exact eigenstates is not practical in the regime of experimental interest, with 1000 particles or more.

This has been the topic of several publications. The first [28] used a multi-configurational time-dependent Hartree method for bosons (MCTDHB) approach with  $N = 1000$  and two spatial modes, predicting a sudden break-up into a pair of equal size fragments. This calculation was recently shown to be not fully converged, violating known quantum center-of-mass (COM) expansion physics [29]. Our results confirm this earlier analysis. The predictions obtained here are completely different, with no evidence of a sudden breakup after a fixed evolution time.

Other approaches have used either exact methods [23], or matrix product states [22]. These were limited in number to  $N < 20$ . Here we investigate larger particle numbers, i.e.,  $N = 10^3 - 10^4$ , and large numbers of independent modes, of order  $10^5$ . This is an experimentally realistic regime. Our calculations preserve all local conservation laws and (nearly) exact COM dynamics, giving results that are both quantitatively and qualitatively different to earlier variational studies.

In one dimensional optical or atomic waveguides, a similar Hamiltonian applies to either massive atomic Bose-Einstein condensate (BEC) experiments or to photonic experiments, where dispersion gives rise to an effective mass. If the bosons are confined to a single transverse mode, one obtains an 1D Bose gas theory, valid for low energies:

$$\hat{H}_{1D} = \frac{\hbar^2}{2m} \int \hat{\Psi}_{1D}^\dagger H_1 \hat{\Psi}_{1D} dr_3 + \frac{g_{1D}}{2} \int \left( \hat{\Psi}_{1D}^\dagger \right)^2 \hat{\Psi}_{1D}^2 dr_3. \quad (1)$$

Here,  $\mathbf{r}$  is the spatial coordinate, with a one-dimensional confinement so the dynamics occur in the  $r_3$  direction. The mass is  $m$ , and for an atomic Bose gas in a parabolic trap one has:

$$\begin{aligned} H_1 &= -\hbar^2 \partial_3^2 / 2m + m\omega_3^2 r_3^2 / 2 \\ g_{1D} &= 2\hbar\omega_\perp a, \end{aligned} \quad (2)$$

where  $a$  is the three-dimensional S-wave scattering length, and the effective transverse trapping frequency of:  $\omega_\perp = \sqrt{\omega_1\omega_2}$ . If the system is photonic or polaritonic, as in a fibre optical experiment [2, 25, 35], the relevant parameters come from the dispersion and optical nonlinearity properties of the fiber.

This can be transformed to dimensionless form by choosing a length scale  $r_0$  and time scale  $t_0$  such that  $r_0^2 = \hbar t_0 / 2m$ . Distance is scaled so that  $z = r_3 / r_0$ , and time is scaled to give a dimensionless time  $\tau = t / t_0$ . The resulting Hamiltonian, in the form introduced by Lieb and Liniger [7], with a dimensionless wave-function  $\hat{\psi} = \sqrt{r_0} \hat{\Psi}_{1D}$ , is:

$$\hat{H} = \int dz \left[ \hat{\psi}_{,z}^\dagger(z) \hat{\psi}_{,z}(z) + C \left( \hat{\psi}^\dagger(z) \right)^2 \hat{\psi}^2(z) \right]. \quad (3)$$

We use a subscript to indicate a derivative, so that:

$$\hat{\psi}_{,z}(z) \equiv \partial_z \hat{\psi}(z) \equiv \frac{\partial}{\partial z} \hat{\psi}(z). \quad (4)$$

Here we note the following translation between the physical and dimensionless units in the case of a trapped Bose-Einstein condensate [11, 37]:

$$\begin{aligned} \hat{H} &= \hat{H}_1 / E_0 \\ E_0 &= \hbar / t_0 = \hbar^2 / 2mr_0^2 \\ C &= \frac{mg_{1D}r_0}{\hbar^2} = 2m\omega_\perp r_0 a / \hbar. \end{aligned} \quad (5)$$

A convenient procedure for solitons is to simply define  $r_0$  as the characteristic initial dimension, so that  $C$  is of the order of the inverse particle number  $N$ .

The corresponding dynamical equation is known as the one-dimensional quantum nonlinear Schrodinger equation. It also describes quantum photonic propagation in one-dimensional optical fibers [31], under similar conditions of tight transverse confinement. Thus, an almost identical picture holds for 1D photonic systems [31, 35], except for additional Raman-Brillouin coupling to phonons, owing to the use of dielectric waveguides [38, 39]. In both the photonic and atomic experiments, there are additional dissipative couplings due to linear and nonlinear losses and phase noise. These effects can lead to additional corrections in the equations. For simplicity, dissipation is ignored here, which leads to some limitations on the possible interaction time.

As usual with Bose fields, the particle density is denoted  $\hat{n}(z) = \hat{\psi}^\dagger(z) \hat{\psi}(z)$ . For numerical calculations we

will assume a momentum cutoff,  $k_C$ . The initial quantum states of either experimental photonic pulses or BECs are typically neither a number nor an energy eigenstate. There is generally a shot-to-shot randomness in the state preparation that results in experimental number fluctuations, because a large number of interacting bosons requires an extremely precise preparation to give a pure number state. It is more common to have at least a Poissonian number variance. Even this may be an underestimate in photonic experiments or in current BEC technology [40] when the atom numbers are larger than  $10^3$ . Accordingly, we assume Poissonian number fluctuations in the calculations given here, in order to represent typical initial quantum density matrices.

The Wigner distribution  $W[\psi]$  over Wigner fields  $\psi$  exists for any quantum state [33, 41]. It is not always positive definite. The usual operator time-evolution equation

$$\frac{d\hat{\psi}}{dt} = -i \left[ \hat{H}, \hat{\psi} \right], \quad (6)$$

where the Hamiltonian  $\hat{H}$  is defined by Eq. (3), can be transformed [42] into a differential equation for  $W[\psi]$ , typically with third or higher order derivatives. After truncation of third order derivatives [24], which are the highest order terms in a  $1/N$  expansion for  $N$  particles, one obtains a second order Fokker-Plank equation for  $W[\psi]$ . This is an approximate functional differential equation for a probability distribution over Wigner fields.

When the evolution is unitary, this results in a partial differential equation for phase-space variables using well-known procedures [25, 26, 43]. The resulting equation for the Wigner field  $\psi$ , is:

$$\frac{d\psi}{dt} = i\nabla^2 \psi - 2iC\psi (|\psi|^2 - 1/\Delta z), \quad (7)$$

where  $\Delta z$  is the lattice spacing or inverse momentum cutoff. Quantum noise is present in the initial conditions. We start from a state with Poissonian number distribution, which is equivalent to a coherent state:

$$\hat{\rho}(t=0) = |\alpha(z)\rangle \langle \alpha(z)|, \quad (8)$$

where  $|\alpha(z)|^2 = n(z)$ . In the Wigner representation this is exactly represented by an ensemble of fields  $\psi(z)$  with initial quantum noise  $\eta_k$ , with

$$\psi(z) = \sqrt{n(z)} + \frac{1}{\sqrt{2}} \sum_k \frac{1}{\sqrt{L}} \eta_k e^{ikz}. \quad (9)$$

Here  $\eta_k$  are complex random numbers correlated as  $\langle \eta_k \eta_{k'}^* \rangle = \delta_{kk'}$ ,  $\langle \eta_k \eta_{k'} \rangle = 0$ . The functional integration over the Wigner distribution is performed by generating multiple random initial states and using them to seed independent integrations of the PDE. This results in a large number,  $N_s$ , of independent field modes — each evolving in time with equal probability.

The Wigner phase-space method generates a direct representation of symmetrically ordered quantum observables. To obtain the usual normally-ordered quantum observables, one must transform the results of a Wigner calculation from a symmetrically ordered to a normally ordered form. This also removes the divergence of symmetrically-ordered observables at large momentum cutoff. The expectation values of symmetrically ordered operator expressions can be obtained by integrating this equation over multiple independent trajectories to produce a set of values  $\psi^{(j)}$  and averaging over a corresponding function of these values.

There is an approximate equality between symmetrically ordered quantum averages and Wigner averages, where the  $N$ -dependent truncation error depends on the evaluated operator [44, 45]:

$$\left\langle \left\{ \hat{O} \left( \hat{\psi}, \hat{\psi}^\dagger \right) \right\} \right\rangle \approx \left\langle \left\{ \hat{O} \right\} \right\rangle_W = \langle O \rangle_W. \quad (10)$$

We consider a quantum dynamical experiment where an initial state is prepared and then evolved in time. The initial state is a Poissonian mixture of uncorrelated particles with mean value  $N = 10^3 - 10^4$  in a localized spatial mode. The equivalent coherent state has the classical soliton shape that occurs with some small initial coupling of  $C_i = -2/N$ , with  $r_0$  as the characteristic initial size, so that in dimensionless units,  $\alpha(z) = \sqrt{N/2} \operatorname{sech}(z)$ .

This corresponds to an ultra-cold atomic Bose gas experiment, with a BEC initially trapped in a localized state with no interactions. At time  $t = 0$ , the interaction Hamiltonian is turned on to a larger value of  $C_f = -8/N$ , allowing particles to interact and forming a breather, a higher-order oscillating soliton. The resulting density profile is shown in Fig. 1 for  $N = 1000$  and in Fig. 2 for  $N = 10000$ . The result of the initial condition is that a high-order soliton or breather is formed [46], with a characteristic period of  $\tau_b = \pi/4$ . Our numerical results show characteristic breathing oscillations such that the mean breather amplitude decays with time.

This simulation is similar to related experimental proposals of first creating a fundamental soliton at weak coupling, then suddenly increasing the coupling strength. The coupling change would be caused by either a pulse entering a fiber in a photonic experiment, or else a change in a tunable Feshbach resonance in an atomic system. A number of different theoretical methods [22, 23, 28] have been used to analyze this type of proposed experiment, making it of topical interest. The present protocol employs a localized non-interacting BEC as the initial state, following earlier proposals [28, 29]. The timescales and numbers used are within the general parameter range achievable with current  ${}^7\text{Li}$  [21] and  ${}^{85}\text{Rb}$  [27] ultra-cold atomic physics experiments.

The simulation is sensitive to the selected spatial and momentum grids. The spatial grid must be symmetrical around 0 and have a point at  $z = 0$ , or else the

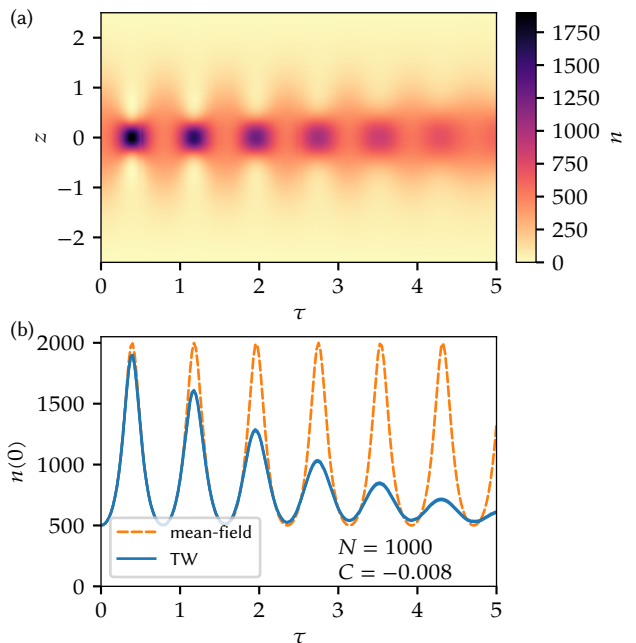


Figure 1. Density near the centre of the simulation area (a) and at  $z = 0$  (b) over time. Simulation with  $N = 10^3$ ,  $C = -8 \times 10^{-3}$ ,  $M = 512$ ,  $L = 20$ ,  $10^5$  trajectories,  $10^5$  time steps. The area between the simulation curves (solid blue lines) denotes the estimated sampling error. The result of the mean-field simulation (dashed orange lines) are shown for comparison. The time-step errors are smaller than the line thickness and are not shown on the graph.

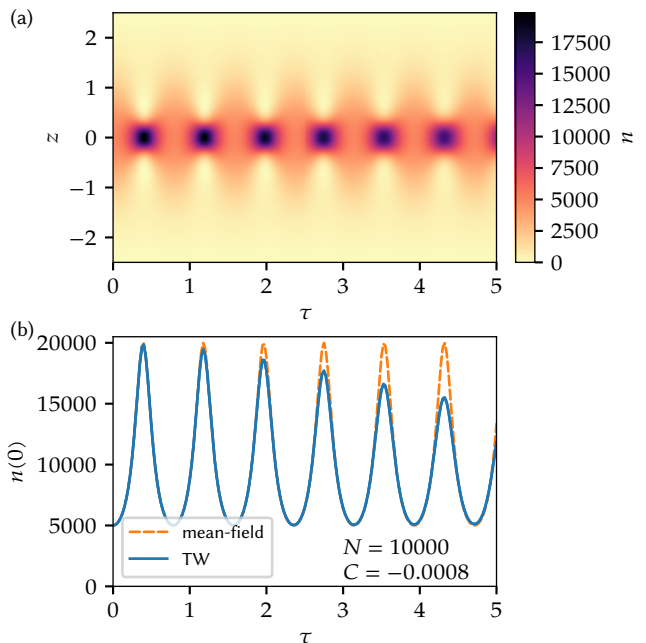


Figure 2. Density near the centre of the simulation area (a) and at  $z = 0$  (b) over time. Simulation with  $N = 10^4$ ,  $C = -8 \times 10^{-4}$ , other properties as in Fig. 1.

decay happens on a faster scale, since there is insufficient lattice resolution for spatial convergence. The momentum grid should ideally be symmetrical around 0, which can be achieved by using a pair of position- and momentum-dependent coefficients applied before and after the Fourier transform. If this condition is not satisfied, the unbalanced high-momentum components of the noise lead to numerical errors. A finite lattice was used with periodic boundary conditions at  $z = \pm L/2$ . Results were obtained using a public domain stochastic partial differential equation code [47] with a fourth-order Runge-Kutta interaction picture algorithm [48], then cross-checked with a larger number of samples using an open source graphical processor unit (GPU) code.

The initial density matrix used here is a random phase mixture of coherent states. As explained above, this is exactly equivalent to a Poissonian mixture of initial pure number states in a single spatial mode, chosen as  $u = \text{sech}(z)/\sqrt{2}$ , similar to previous investigations [28, 29]. Since the measurements phase-independent, only a single phase in the mixture is calculated. Averaging over phases would produce identical results in every input phase.

While a pure state initial condition is sometimes used theoretically, it is less compatible with experiments. These employ a mixture of initial boson numbers [40] with at least Poissonian number fluctuations. In the present examples, the initial boson number is  $N = N \pm \sqrt{N}$ , where  $N = 10^3 - 10^4$ . The number standard deviation is  $\pm\sqrt{N}$ , or  $\pm 1\% - 3.2\%$ , which is of the order of, or less than typical standard deviations for these types of experiment.

The sampling errors can be reduced by taking more samples, and are smaller than expected experimental uncertainties in such measurements. Convergence tests were carried out with the four exact conservation laws,  $\hat{N}$ ,  $\hat{P}$ ,  $\hat{H}$ ,  $\hat{H}_3$  [49], and with exact COM expansion predictions [50, 51]. All agreed with the predicted conserved behavior within sampling error, apart from small errors of size  $N^{-3/2}$ . The comparison with these tests will be reported in detail elsewhere. This is not a guarantee of exactness, as truncated Wigner methods have a growing truncation error with time [52, 53]; however, earlier variational results were not able to satisfy these tests [29] in this regime of mesoscopic particle number. The main issue is whether the breather behaves classically, or whether the oscillations are damped owing to quantum fragmentation of the higher-order soliton. This problem is extremely challenging in quantum many-body theory, as it involves exponentially many eigenstates. As can be seen by the results given here, in the TW approximation the oscillations are predicted to decay nearly exponentially, without sudden fragmentation as predicted using variational methods [28].

Since the center-of mass position is known to spread, one may expect that the on-axis density plotted in Fig. 1 and Fig. 2 might decay purely due to the quantum uncer-

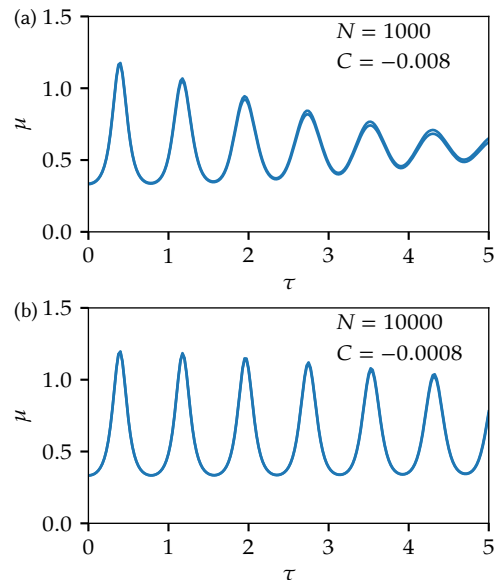


Figure 3. Correlation  $\mu$  over time. Simulation with  $N = 10^3$ ,  $C = -8 \times 10^{-3}$  (a) and  $N = 10^4$ ,  $C = -8 \times 10^{-4}$  (b),  $M = 512$ ,  $L = 20$ ,  $10^5$  trajectories,  $10^5$  time steps. The area between the simulation curves (solid blue lines) denotes the estimated sampling error. The time-step errors are smaller than the line thickness and are not shown on the graph.

tainty in the final position. Therefore, in Fig. 3, we introduce the dimensionless Glauber second order correlation function,  $G^{(2)}(z_1, z_2) = \langle \hat{\psi}^\dagger(z_1) \hat{\psi}^\dagger(z_2) \hat{\psi}(z_2) \hat{\psi}(z_1) \rangle$ , and investigate the integrated correlation:

$$\mu = \int G^{(2)}(z, z) dz / N^2. \quad (11)$$

This integrated correlation function measures the “peakedness” of a spatial distribution, in a way that is independent of the location of the peak. We see that this also decays, although not as strongly as the on-axis density. We conclude that the breather gradually radiates or fragments due to quantum effects with increasing similarity to mean field behaviour as  $N \rightarrow \infty$ .

In summary, our results predict continuous quantum fragmentation of higher-order soliton breathers at particle numbers of  $N = 1000$ , with results closer to mean field predictions at  $N = 10000$ . This is readily testable in BEC experiments.

We would like to acknowledge helpful discussions with J. Brand, J. Cosme, R. Hulet, B. Malomed, M. Olshanii and L. Carr. This work was performed in part at Aspen Center for Physics, which is supported by National Science Foundation grant PHY-1607611.

[1] M. Rosenbluh and R. M. Shelby, Phys. Rev. Lett. **66**, 153 (1991).

- [2] P. D. Drummond, R. M. Shelby, S. R. Friberg, and Y. Yamamoto, *Nature* **365**, 307 (1993).
- [3] J. Heersink, V. Josse, G. Leuchs, and U. L. Andersen, *Opt. Lett.* **30**, 1192 (2005).
- [4] J. F. Corney, P. D. Drummond, J. Heersink, V. Josse, G. Leuchs, and U. L. Andersen, *Phys. Rev. Lett.* **97**, 023606 (2006).
- [5] M. Egorov, R. P. Anderson, V. Ivannikov, B. Opanchuk, P. Drummond, B. V. Hall, and A. I. Sidorov, *Phys. Rev. A* **84**, 021605 (2011).
- [6] H. B. Thacker, *Reviews of Modern Physics* **53**, 253 (1981).
- [7] E. H. Lieb and W. Liniger, *Physical Review* **130**, 1605 (1963).
- [8] J. B. McGuire, *Journal of Mathematical Physics* **5**, 622 (1964).
- [9] D. M. Gangardt and G. V. Shlyapnikov, *Phys. Rev. Lett.* **90**, 010401 (2003).
- [10] K. Kheruntsyan, D. Gangardt, P. Drummond, and G. Shlyapnikov, *Physical review letters* **91**, 040403 (2003).
- [11] K. Kheruntsyan, D. Gangardt, P. Drummond, and G. Shlyapnikov, *Physical Review A* **71**, 053615 (2005).
- [12] B. L. Tolra, K. O'hara, J. Huckans, W. D. Phillips, S. Rolston, and J. V. Porto, *Physical review letters* **92**, 190401 (2004).
- [13] T. Kinoshita, T. Wenger, and D. S. Weiss, *Phys. Rev. Lett.* **95**, 190406 (2005).
- [14] T. Langen, S. Erne, R. Geiger, B. Rauer, T. Schweigler, M. Kuhnert, W. Rohringer, I. E. Mazets, T. Gasenzer, and J. Schmiedmayer, *Science* **348**, 207 (2015).
- [15] M. Rigol, V. Dunjko, V. Yurovsky, and M. Olshanii, *Physical review letters* **98**, 050405 (2007).
- [16] L. Khaykovich, F. Schreck, G. Ferrari, T. Bourdel, J. Cubizolles, L. D. Carr, Y. Castin, and C. Salomon, *Science* **296**, 1290 (2002).
- [17] K. Strecker, G. Partridge, A. Truscott, and R. Hulet, *Nature* **417**, 150 (2002).
- [18] P. Medley, M. Minar, N. Cizek, D. Berryrieser, and M. Kasevich, *Physical review letters* **112**, 060401 (2014).
- [19] G. D. McDonald, C. C. Kuhn, K. S. Hardman, S. Bennetts, P. J. Everitt, P. A. Altin, J. E. Debs, J. D. Close, and N. P. Robins, *Physical review letters* **113**, 013002 (2014).
- [20] J. H. Nguyen, P. Dyke, D. Luo, B. A. Malomed, and R. G. Hulet, *arXiv preprint arXiv:1407.5087* (2014).
- [21] J. H. Nguyen, D. Luo, and R. G. Hulet, *Science* **356**, 422 (2017).
- [22] C. Weiss and L. D. Carr, *arXiv preprint arXiv:1612.05545* (2016).
- [23] V. A. Yurovsky, B. A. Malomed, R. G. Hulet, and M. Olshanii, *arXiv preprint arXiv:1706.07114* (2017).
- [24] R. Graham, *Quantum Statistics in Optics and Solid-State Physics*, edited by G. Hohler, Vol. 66 (Springer, New York, 1973) p. 1.
- [25] P. D. Drummond and A. D. Hardman, *Europhysics Letters (EPL)* **21**, 279 (1993).
- [26] M. Steel, M. K. Olsen, L. I. Plimak, P. D. Drummond, S. Tan, M. J. Collett, D. Walls, and R. Graham, *Physical Review A* **58**, 4824 (1998).
- [27] P. Everitt, M. Sooriyabandara, M. Guasoni, P. Wigley, C. Wei, G. McDonald, K. Hardman, P. Manju, J. Close, C. Kuhn, *et al.*, *arXiv preprint arXiv:1703.07502* (2017).
- [28] A. I. Streltsov, O. E. Alon, and L. S. Cederbaum, *Physical review letters* **100**, 130401 (2008).
- [29] J. G. Cosme, C. Weiss, and J. Brand, *Physical Review A* **94**, 043603 (2016).
- [30] T. Tao, *Nonlinear dispersive equations: local and global analysis*, 106 (American Mathematical Soc., 2006).
- [31] S. J. Carter, P. D. Drummond, M. D. Reid, and R. M. Shelby, *Phys. Rev. Lett.* **58**, 1841 (1987).
- [32] Y. Lai and H. Haus, *Physical Review A* **40**, 854 (1989).
- [33] E. P. Wigner, *Phys. Rev.* **40**, 749 (1932).
- [34] R. J. Glauber, *Phys. Rev.* **131**, 2766 (1963).
- [35] P. Drummond and S. Carter, *JOSA B* **4**, 1565 (1987).
- [36] J. F. Corney, J. Heersink, R. Dong, V. Josse, P. D. Drummond, G. Leuchs, and U. L. Andersen, *Phys. Rev. A* **78**, 023831 (2008).
- [37] M. Olshanii, *Physical Review Letters* **81**, 938 (1998).
- [38] J. P. Gordon, *Optics letters* **11**, 662 (1986).
- [39] S. Carter and P. Drummond, *Physical review letters* **67**, 3757 (1991).
- [40] C.-S. Chuu, F. Schreck, T. P. Meyrath, J. Hanssen, G. Price, and M. Raizen, *Physical review letters* **95**, 260403 (2005).
- [41] M. Hillery, R. F. O'Connell, M. O. Scully, and E. P. Wigner, *Physics reports* **106**, 121 (1984).
- [42] J. Moyal, *Proceedings of the Cambridge Philosophical Society* **45**, 99 (1949).
- [43] B. Opanchuk and P. D. Drummond, *Journal of Mathematical Physics* **54**, 042107 (2013).
- [44] P. Kinsler, M. Fernée, and P. Drummond, *Physical Review A* **48**, 3310 (1993).
- [45] P. Kinsler, *Phys. Rev. A* **53**, 2000 (1996).
- [46] P. Wai, C. R. Menyuk, Y. Lee, and H. Chen, *Optics letters* **11**, 464 (1986).
- [47] S. Kiesewetter, R. Polkinghorne, B. Opanchuk, and P. D. Drummond, *SoftwareX* **5**, 12 (2016).
- [48] B. M. Caradoc-Davies, *Vortex dynamics in Bose-Einstein condensates*, Ph.D. thesis (2000).
- [49] B. Davies, *Physica A: Statistical Mechanics and its Applications* **167**, 433 (1990).
- [50] W. Kohn, *Physical Review* **123**, 1242 (1961).
- [51] T. Vaughan, P. Drummond, and G. Leuchs, *Physical Review A* **75**, 033617 (2007).
- [52] A. Sinatra, C. Lobo, and Y. Castin, *Journal of Physics B: Atomic, Molecular and Optical Physics* **35**, 3599 (2002), *arXiv:condmat/0201217*.
- [53] P. P. Deuar and P. D. Drummond, *Phys. Rev. Lett.* **98**, 120402 (2007).